# Pigment structure in the light-harvesting protein of the siphonous green alga Codium fragile

Simona Streckaité, Manuel J. Llansola-Portoles, Andrew A. Pascal, Cristian Ilioaia, Andrew Gall, Soichiro Seki, Ritsuko Fujii, Bruno Robert

# Pigment structure in the light-harvesting protein of the siphonous green alga *Codium fragile*

Simona Streckaite[a], Manuel J. Llansola-Portoles[a], Andrew A. Pascal[a], Cristian Ilioaia[a], Andrew Gall[a], Soichiro Seki[b], Ritsuko Fujii[b,c], Bruno Robert[a*]

[a] Université Paris-Saclay, CEA, CNRS, Institute for Integrative Biology of the Cell (I2BC), 91198, Gif-sur-Yvette, France
[b] Osaka City University, Graduate School of Science, Sumiyoshi Ku, 3-3-138 Sugimoto, Osaka 5588585, Japan
[c] Osaka City University, The OCU Research Center for Artificial Photosynthesis, Sumiyoshi Ku, 3-3-138 Sugimoto, Osaka 5588585, Japan

*Corresponding author: bruno.robert@cea.fr

## Abstract

The siphonaxanthin-siphonein-chlorophyll-*a*/*b*-binding protein (SCP), a trimeric light-harvesting complex isolated from photosystem II of the siphonous green alga *Codium fragile*, binds the carotenoid siphonaxanthin (Sx) and/or its ester siphonein in place of lutein, in addition to chlorophylls *a*/*b* and neoxanthin. SCP exhibits a higher content of chlorophyll *b* (Chl-*b*) than its counterpart in green plants, light-harvesting complex II (LHCII), increasing the relative absorption of blue-green light for photosynthesis. Using low temperature absorption and resonance Raman spectroscopies, we reveal the presence of two non-equivalent Sx molecules in SCP, and assign their absorption peaks at 501 and 535 nm. The red-absorbing Sx population exhibits a significant distortion that is reminiscent of lutein 2 in trimeric LHCII. Unexpected enhancement of the Raman modes of Chls-*b* in SCP allows an unequivocal description of seven to nine non-equivalent Chls-*b,* and six distinct Chl-*a* populations in this protein.

**Keywords**. siphonaxanthin, SCP, siphonous green algae, *Codium fragile*, resonance Raman, siphonein

## 1. Introduction

During photosynthesis, plants, algae and some bacteria convert energy received from sunlight into highly energetic compounds using membrane-embedded pigment-protein complexes. In this process, the energy of solar photons is gathered by light-harvesting complexes (LHCs) and transferred in the form of excitation energy to reaction centres (RCs), where it is converted into electrochemical energy by charge separation. LHCs are diverse, reflecting the adaptation of photosynthetic organisms to their specific light environment to optimise photosynthetic efficiency. In addition to chlorophyll (Chl), which is the active pigment for excitation energy transfer from complex to complex, photosynthetic proteins generally contain carotenoid molecules, which harvest light in the blue-green spectral range and transfer this energy to Chl molecules, as well as playing a crucial role in photoprotection [1,2]. The major LHC from higher plants, the trimeric protein LHCII, binds 14 Chls (8 Chls-*a* and 6 Chls-*b*) and 4 carotenoid molecules (2 non-equivalent luteins, 1 9'-*cis* neoxanthin (Neo) and 1 violaxanthin or zeaxanthin) per monomer [3]. Land plants share the same photosynthetic pigment-protein system, while algae have developed a variety of light-harvesting systems, reflecting both the diversity of their origin and the variety of their light environments [4–6]. Major carotenoids for light-harvesting in marine algae are the allenic xanthophylls fucoxanthin (Fx) and peridinin (Per), the former mainly in brown algae and diatoms [7–9], and the latter in dinoflagellates [10]. Antenna proteins in both cases (fucoxanthin-chlorophyll-protein, FCP, and peridinin-chlorophyll-protein, PCP, respectively) bind carotenoids at higher relative stoichiometries [9] in order to increase the ability of these organisms to harvest photons in the blue-green range [11,12]. This is supplemented by the presence of Chl-*c* in these complexes, a chlorophyll pigment with intense absorption in the Soret region. Marine LHCs have received significant attention in recent years, in part because of these differences in structure and function relative to plant LHCs. Their study may in particular yield insight into the key mechanisms underlying antenna optimisation to light quality.

Siphonous algae are primitive green algae based on an original architecture: they are unicellular, composed of huge cells in which nuclei divide (termed coenocytic algae). Contrary to other green algae, they mainly contain α-carotene but no

β-carotene [13]. Siphonous algae possess specific antenna proteins of the LHC family, binding both Chl-*a* and Chl-*b*, 9'-*cis* Neo and, in place of lutein, siphonaxanthin and/or its esterified form siphonein [12,14–16] (see Fig. 1). The stoichiometry of Chl-*b* bound to their PSII light-harvesting complex is also higher than

in plant LHCII. A Chl-*b* : Chl-*a* ratio of 8 : 6 was determined from HPLC studies on the PSII light-harvesting complex isolated from the siphonous green algae *Bryopsis (B.) maxima* [17] and *B. corticulans* [12,18].

In this manuscript, we use low temperature absorption and resonance Raman (RR) to investigate pigment structure in the trimeric PSII light-harvesting complex purified from the siphonous green alga *Codium* (*C.*) *fragile* (siphonaxanthin-siphonein-Chl-*a*/*b*-protein, SCP). Both the presence of Sx and the higher number of Chl-*b* molecules enhance the absorption in the 460-540 nm region in these SCPs, as compared to plant LHCs [19], thus extending their light-harvesting capacity into the blue-green region [14,15,20].

## 2. Materials and methods

*C. fragile* (KU-0654, KU-MACC, Kobe, Japan) was cultivated at 22 °C with continuous air bubbling under white fluorescent light (6-9 µmol photon $m^{-2}s^{-1}$) in $ASP_{12}$ medium [21] with minor modifications: sodium metasilicate was removed, and Tris was replaced by HEPES. Sodium nitrate, vitamin $B_{12}$ (cyanocobalamin), biotin, and thiamine-HCl were enhanced 4-, 7.5-, 1.5- & 2-fold, respectively. In addition, vitamins, including sodium nitrate, disodium grycerophosphate, potassium phosphate, vitamin $B_{12}$, biotin, thiamine-HCl, were added directly to the medium every three days. Harvested cells were lyophilized and ground to a powder, from which thylakoid membranes were isolated according to [14]. Thylakoids were solubilized with 1 % (w/v) n-dodecyl-β-D-maltopyranoside (β-DDM, Kishida Chemical Co. Ltd., Osaka, Japan) at 4 °C for one hour. After centrifugation for 30 minutes at 4 °C (19k rpm, R20A2 rotor, CR22GIII, Hitachi Koki Co., Ltd., Ibaraki, Japan), the supernatant was injected onto an ion-exchange column (DEAE TOYOPEARL 650S, 2.2 cm i.d. × 20 cm, Tosoh Corporation, Yamaguchi, Japan). This column was subjected to a linear 0-1 M NaCl gradient in 20 mM Tris-HCl pH 7.2, 0.03 % β-DDM (w/v) using an FPLC system (ÄKTApure, GE Healthcare Japan, Tokyo, Japan), and major fractions were collected. Protein content and purity was assessed by SDS-PAGE (Mini-Protean TGX precast gels 12%, Bio-Rad, Hercules, CA, USA; Fig. S1); fractions 2 and 3, containing trimeric SCP, were pooled for further analysis.

Pigments were extracted from desalted SCP solutions as described previously [22]. 1 µL extract was injected into the HPLC system (UHPLC, Nexera XR with a SIL-30Ac auto sampler and a SPD-M10Avp, Shimadzu, Kyoto, Japan), using a reversed-phase ODS column (Cosmosil 2.5C18-MS-II, 3.0 ID x 75 mm). A linear gradient of eluent A (methanol : acetonitrile : water, 9:7:4, v/v/v) to eluent B (acetonitrile : ethyl

acetate, 3:7, v/v) was performed from 2 to 10 min after injection, at a flow rate of 1.33 mL/min. Pigment composition was calculated using molar extinction coefficients as described in [16]; standard errors were calculated for three replicates.

Siphonaxanthin was isolated from *Codium* (*C.*) *intricatum* cultivated in filamentous form (a gift from Dr. Iha, South Product Co. Ltd. Okinawa, Japan) [16]. Lyophilized *C. intricatum* was ground with a chilled mixture of methanol and acetone. The supernatant was saponified overnight at 4 °C by adding KOH at a final concentration of 8 % (w/v). Pigments were collected with dichloromethane and washed with water, and their purity was confirmed using binary HPLC as in [16].

FCP was isolated from the brown alga *Laminaria saccharina* by iso-electric focussing, as described in [23]. LHCII was isolated from spinach by a sucrose gradient of β-DDM-solubilised PSII membranes, as described in [24].

UV-VIS Absorption spectra were measured using a Varian Cary E5 Double-beam scanning spectrophotometer (Agilent), with a 1.0-cm path-length cuvette. Low temperature measurements were performed in a helium bath cryostat (Maico Metriks, Tartu, Estonia); 60 % glycerol (v/v) was added to the sample to prevent devitrification.

Resonance Raman spectra were recorded at 77 K in a liquid nitrogen (LN2) flow cryostat (Air Liquide, France). Laser excitations at 413.1 nm, at 457.9, 488.0, 501.7, 514.5 & 528.7 nm, and at 561.0 nm were obtained with Coherent $Kr^+$ (Innova 90), $Ar^+$ (Sabre) and OBIS lasers, respectively. Excitation at 441.6 nm was obtained with a He-Cd laser (Liconix). Output laser powers of 10–100 mW were attenuated to < 5 mW at the sample. Scattered light was collected at 90° to the incident light, and focused into a Jobin-Yvon U1000 double-grating spectrometer (1800 grooves/mm), equipped with a red-sensitive, back-illuminated, LN2-cooled CCD camera. Sample stability and integrity was assessed based on the similarity between the first and last Raman spectra.

## 3. Results and discussion

### *3.1. Pigment Composition*

The pigment composition of *C. fragile* SCP is shown in Table 1 (example HPLC profile in Fig. S2), and is essentially the same as that of SCP isolated from *B. corticulans* [12]. The molecular structures of Sx, Sn and 9'-*cis* Neo [16] are shown in Fig. 1, together with that of lutein for comparison. Note that Sx and its ester, Sn, have identical conjugated chemical structure, and so they are expected to exhibit similar

spectroscopic properties. Both molecules will therefore be referred to as Sx for the discussion of their absorption and resonance Raman properties.

Table 1. Pigment composition of SCP from *C. fragile.*

| Chl *a*/*b* | Chl-*a* | Chl-*b* | 9'-*cis* Neo | Sx | Sn |
|---|---|---|---|---|---|
| 0.78 | 6.1 ± 0.1 | 7.9 ± 0.1 | 0.90 ± 0.02 | 1.5 ± 0.1 | 0.99 ± 0.01 |

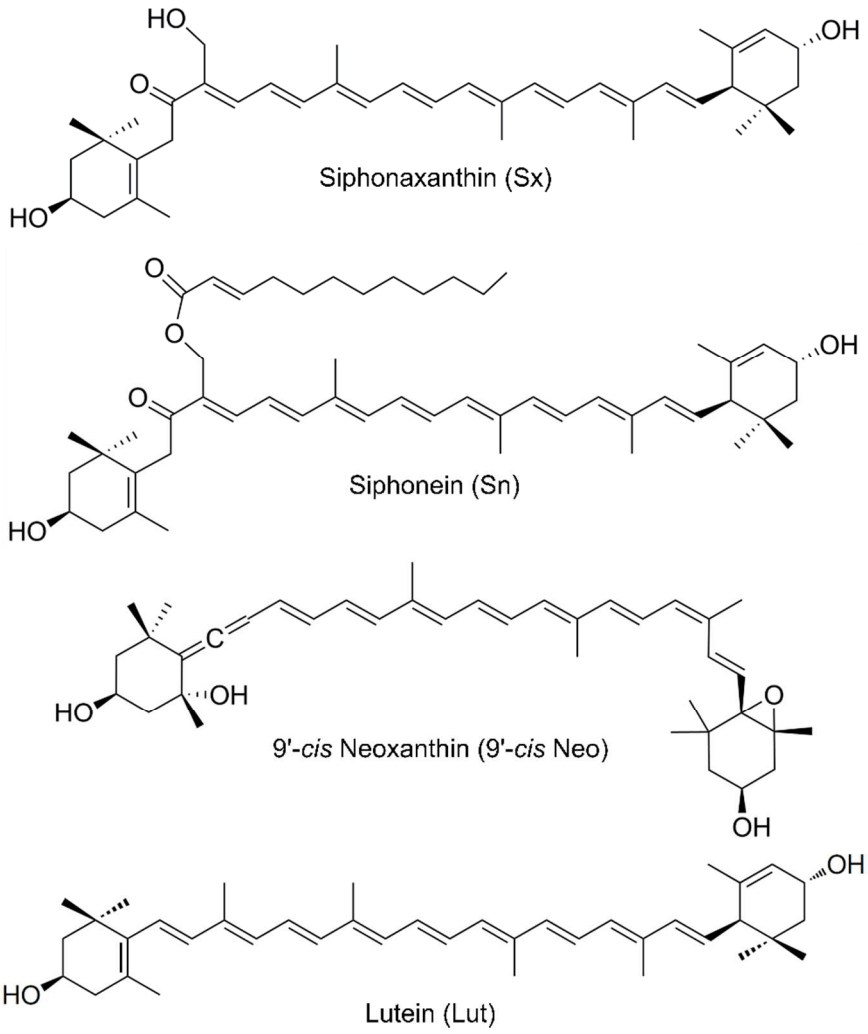


Fig. 1. Molecular structures of carotenoids siphonaxanthin and siphonein. Neoxanthin and lutein are shown for comparison.

*3.2. Absorption spectroscopy*

The absorption spectrum of siphonaxanthin in pyridine at room temperature (RT) is shown in Fig. 2 (blue line). Carotenoids typically exhibit three absorption transitions, corresponding to the 0-0, 0-1 and 0-2 vibrational sublevels of the $S_0$-$S_2$ electronic transition. These vibronic peaks are poorly-defined in the absorption spectrum of Sx, but they can be localised by second derivative analysis (inset to Fig. 2) at 488.0, 457.0 and 428.4 nm (0-0, 0-1 & 0-2 respectively).

In the absorption spectrum of *C. fragile* SCP at RT (green line), the carotenoid transitions are broad and nearly structure-less. They peak at *ca*. 473 nm, with a long tail on the red side. Chl absorption peaks are also broad, peaking at 439, 652 and 672 nm. These transitions can be attributed primarily to Chl-*a* and -*b* Soret, Chl-*b* $Q_y$, and Chl-*a* $Q_y$ bands, respectively. To analyse the contributions of each species more precisely, we measured the absorption spectrum at 4.2 K (Fig. 2, red line). From second derivative analysis (Fig. 2, inset), six contributions can be observed in the blue-green region - at 462, 473, 482, 489, 501 and 535 nm (black arrowheads). The 535 nm band has been previously observed in the chloroplasts and purified LHCs of siphonous green algae, and it is considered to be an index of intactness of the antenna complex [25,26]. At least five carotenoid bands contribute in the 470-535 nm region, suggesting the presence of at least two different carotenoid populations. Contributions at *ca.* 440 nm correspond to the Chl-*a* Soret transition, while that of Chl-*b* is ca. 460 nm [27]. The Chl-*a* $Q_y$ band displays a main peak at 676 nm and a secondary, blue-shifted peak at 671 nm. The intense contribution at 650 nm is unequivocally attributed to the Chl-*b* $Q_y$ region, while the band at 660 nm could originate from Chl-*a* or Chl-*b* (or both). Altogether, the pattern of absorption observed at RT in SCP is similar to that of the SCP from another siphonous green alga, *B. corticulans* [12,18] (see also Table S1). It also appears somewhat similar to LHCII from higher plants [28,29], but with a higher Chl-*b* contribution (as expected from the Chl-*a*/*b* ratio; see Table 1).

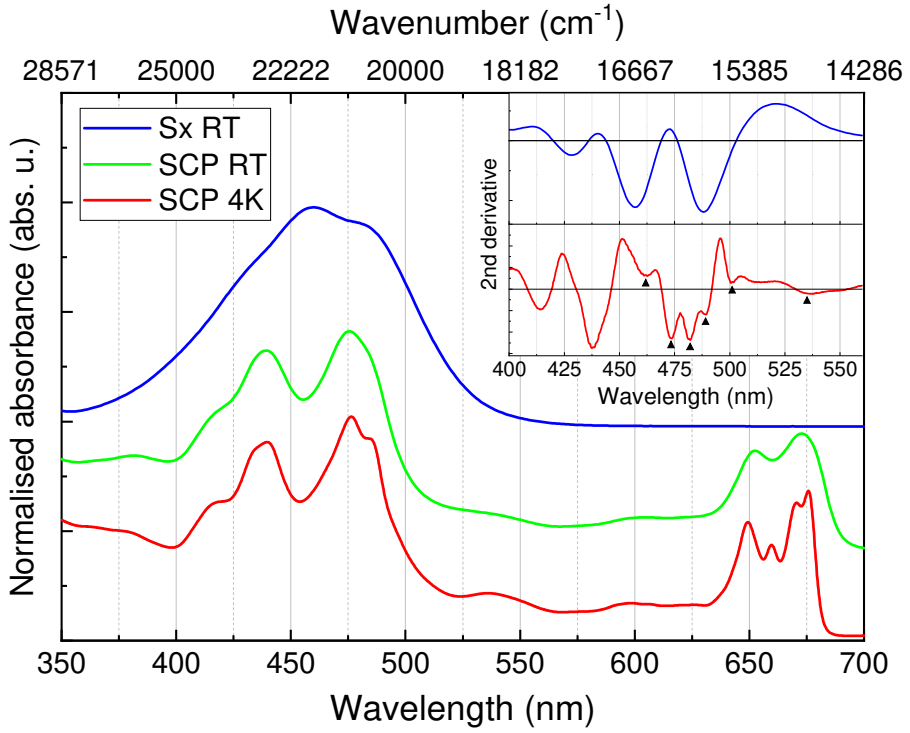


Fig. 2. Room temperature (RT) and 4.2 K absorption spectra of SCP (green and red, respectively), along with that of Sx in pyridine at RT (blue). Inset: second derivative of Sx at RT and SCP at 4.2 K, in the blue-green range.

### *3.3. Resonance Raman of carotenoid molecules in SCP*

In resonance Raman spectroscopy, matching the energy of the excitation light with the electronic transition of a given molecule induces an increase in intensity for those vibrational modes of the molecule that are coupled to the transition (resonance effect). This enables the observation of each class of pigment in pigment-protein complexes [30,31]. Selectivity increases at low temperature, as the bands arising from the electronic transitions become narrower. Thus resonance Raman studies on photosynthetic complexes are generally performed at liquid nitrogen temperatures. Carotenoids display a particularly large resonance Raman cross-section, and their signal dominates the spectra for excitations between 450 and 600 nm [30]. It has been shown that scanning the carotenoid absorption region with the excitation wavelength used may allow the selective observation of each carotenoid population in LHCs [31–33]. This methodology has been extensively applied to compare the structure of the different carotenoid populations bound to these complexes, and to assign the observed absorption maxima to specific carotenoid species [7,34–36].

Carotenoid resonance Raman spectra contain four main groups of bands, called $v_1$-$v_4$, with each region providing specific information on the conformation and/or configuration of the carotenoid involved. In the high-frequency region, the intense $v_1$ band around 1500-1530 $cm^{-1}$ arises from stretching vibrations of the conjugated C=C bonds in the polyene chain, and its precise frequency depends on the effective conjugation length of the molecule [37]. The group of bands around 1160 $cm^{-1}$, called $v_2$, arises from stretching vibrations of C-C bonds coupled with C-H in-plane bending modes. These modes constitute a fingerprint region for determining carotenoid isomerization states (*trans*/*cis*) [38]. The $v_3$ bands, arising from a combination of in-plane rocking vibrations of methyl groups attached to the conjugated chain and in-plane bending modes of the adjacent C-H groups, appear around 1000 $cm^{-1}$, and are a fingerprint of the conjugated end-cycle conformation [39,40]. Finally, the $v_4$ region around 960 $cm^{-1}$ arises from out-of-plane wagging motions of the C-H groups coupled with C-C torsion of the polyene chain [39,41]. As these modes are poorly coupled with the in-plane electronic $S_0$-$S_2$ transition of the molecule, their intensity yields information about the planarity of the C=C conjugated chain.

77 K resonance Raman spectra in the $v_1$ and $v_2$ regions are shown in Fig. 3 for Sx and 9'-*cis* Neo in pyridine, excited at 528 and 488 nm, respectively (upper panel). The spectra of the isolated carotenoids were identical at all excitations in the 514-561 nm region (data not shown). The $v_1$ band is upshifted in Neo spectra relative to Sx, while larger differences are observed in the structure of the $v_2$ region. This latter region for Sx contains a main band at 1161 $cm^{-1}$ with two satellites at 1188 and 1216 $cm^{-1}$, while Neo exhibits the main vibrational mode at 1155 $cm^{-1}$ with satellite bands on the high-frequency side at 1183, 1203 and 1216 $cm^{-1}$. The $v_2$ region of Neo also contains two modes on the low-frequency side at *ca.* 1120 and 1133 $cm^{-1}$, reflecting the 9'-*cis* configuration of this carotenoid [42].

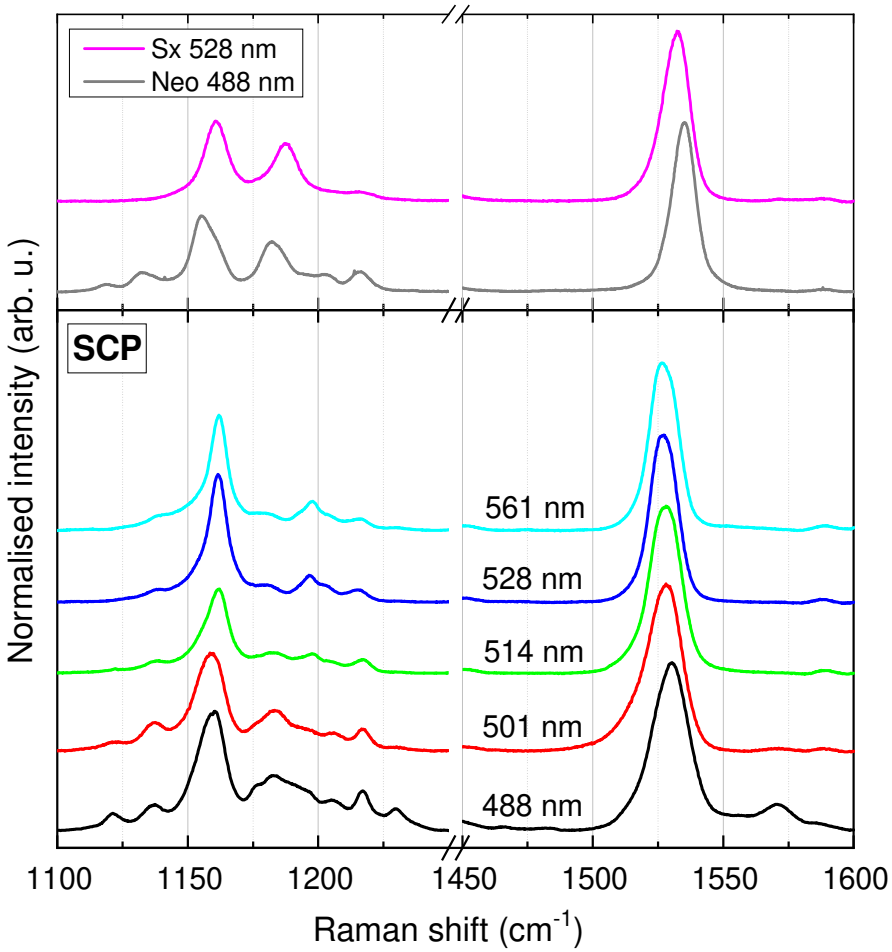


Fig. 3. Resonance Raman spectra at 77 K in $\nu_1$ and $\nu_2$ regions. Upper panel: Sx and Neo in pyridine, excited at 528.7 and 488 nm, respectively. Lower panel: SCP excited at 488.0, 501.7, 514.5, 528.7 and 561.0 nm.

Also shown in Fig. 3 are the $\nu_1$ and $\nu_2$ regions of 77 K resonance Raman spectra of isolated SCP, for excitations in the 488-561 nm range (lower panel). The frequency of the $\nu_1$ band appears to vary according to the excitation wavelength: 1530 $cm^{-1}$ (488.0 nm), 1528 $cm^{-1}$ (501.7 nm), 1528 $cm^{-1}$ (514.5 nm), 1527 $cm^{-1}$ (528.7 nm), and 1526 $cm^{-1}$ (561.0 nm). An additional band at 1571 $cm^{-1}$ is detected upon 488.0 nm excitation, which we do not attribute to carotenoid (see below). At 488.0 and 501.7 nm, the $\nu_2$ region of SCP resembles that of isolated Neo – exhibiting in particular the signature bands for 9'-*cis* isomerization at *ca.* 1120 & 1137 $cm^{-1}$. At 488 nm the $\nu_1$ band is narrower, and observed at 1530 $cm^{-1}$, while at 501.7 nm, it is downshifted and broader. We thus conclude that Neo contributions dominate the signal at 488 nm, while at 501.7 nm the spectra arise from a mixing of Neo and Sx contributions. At longer wavelengths, the Neo contributions in the $\nu_2$ region become

negligible, and the $v_1$ downshifts – indicating that Sx contributions dominate at 514.5 nm and above. However, the $v_1$ band continues to downshift as the excitation shifts further to the red, suggesting the presence of two non-equivalent siphonaxanthin molecules in SCP. One Sx population would have a red-shifted absorption, and could therefore be responsible for the absorption band at 535 nm, while the other would absorb at 501 nm (see Fig. 2).

Figure 4 shows 77 K resonance Raman spectra in the $v_3$ and $v_4$ regions of SCP excited at 488.0, 501.7, 514.5, 528.7 and 561.0 nm, and of Sx and Neo, excited at 528.7 and 488 nm, respectively. Both isolated carotenoids exhibit two broad bands in the $v_3$ range – at 1009 and 1022 $cm^{-1}$ for Sx, and at 1005 and 1024 $cm^{-1}$ (with a shoulder at *ca.* 1020 $cm^{-1}$) for Neo (Fig. 4, right). No clear bands can be observed for Sx in the $v_4$ region, while Neo exhibits a broad, low-intensity contribution only (inset in Fig. 4, right). For 488.0-nm excitation (favouring Neo), SCP spectra exhibit splitting of the 1005 $cm^{-1}$ $v_3$ band, and two bands in the $v_4$ region at 956 and 966 $cm^{-1}$ (a situation reminiscent of Neo bound to plant LHCs, such as LHCII trimers [35]). For excitations to the red (528 and 561 nm), favouring Sx, $v_4$ contains three components at 955, 966 and 973 $cm^{-1}$, but only two when exciting at 501 and 514 nm. The $v_3$ region also displays different patterns at these two excitations. Summation of the 501.7-nm signal with 0.8 of that obtained at 528.7 nm (after normalisation to $v_1$) results in a spectrum almost identical to that obtained at 514.5 nm (501 + 528 nm, Fig. 4). This suggests that the signal obtained at 514.5 nm is not due to a single carotenoid, but rather to a linear combination of the carotenoid populations contributing at 501.7 and 528.7 nm. These results confirm the existence of two non-equivalent Sx molecules in SCP, with the red-absorbing one being more distorted. It is worth noting that the $v_4$ features of the two non-equivalent Sx molecules are strikingly similar to those of the two luteins in LHCIIb trimers [36]. Indeed, $v_4$ reveals that the red-shifted Sx molecule experiences a significant twisting of the carbon skeleton, reminiscent of the red-shifted lutein in LHCII site L2 [36,43]. However, in LHCII, the difference in absorption between the two luteins was associated with a shift of the C=C stretching mode by 4 $cm^{-1}$. It was concluded to arise from the different effective conjugation lengths of the luteins resulting in different conformations [37]. In SCP, the shift of the C=C stretching mode between both Sx molecules is much less (2 $cm^{-1}$), and cannot by itself account for the observed red-shift in absorption. Siphonaxanthin displays a more complex electronic structure, involving intramolecular charge-transfer (ICT) states, and the fine-tuning of these is probably, at least in part, at the origin of the absorption difference between the two Sx molecules in SCP.

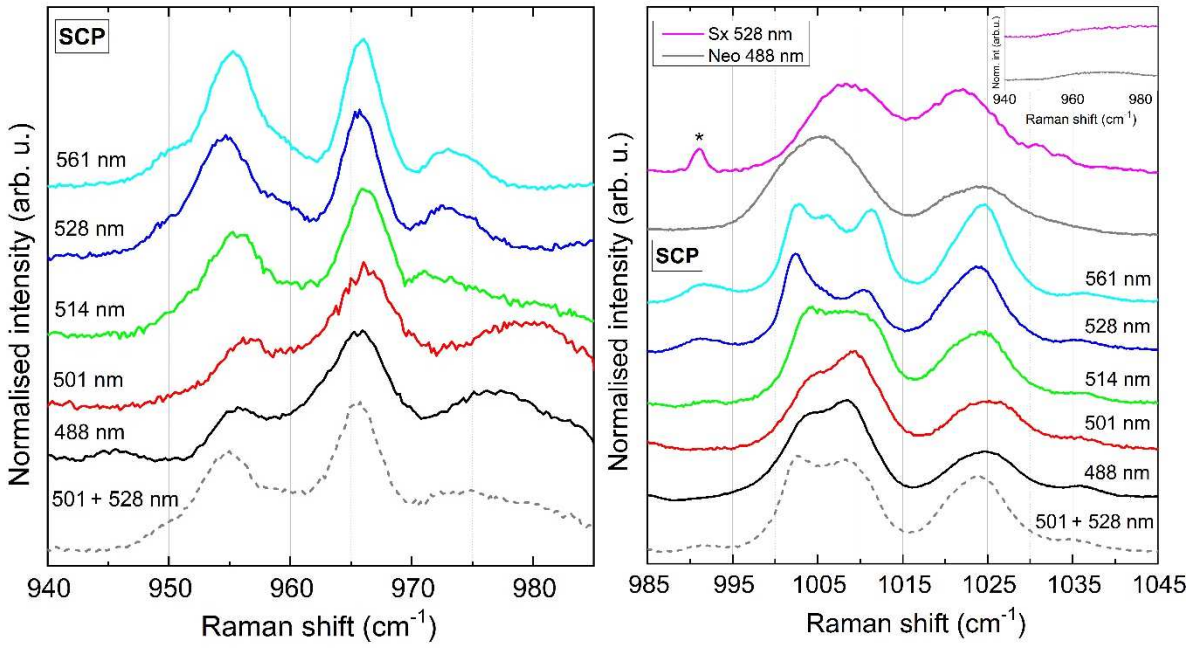


Fig. 4. Resonance Raman spectra at 77 K in $\nu_4$ (left) and $\nu_3$ (right) regions of SCP, excited at 488.0, 501.7, 514.5, 528.7 and 561.0 nm. Also shown is the sum between 501.7 nm and 0.8×528.7 nm ($\nu_1$-normalised spectra; dashed lines). Top spectra on the right: Sx and Neo in pyridine, excited at 528.7 and 488 nm, respectively; Inset: $\nu_4$ region of these spectra. *solvent band

### *3.4. Resonance effects in Raman spectra of SCP*

Classically, in chlorophyll-carotenoid systems like LHCs, Chl-*a* contributions may be observed by exciting at 406.7 and 413.1 nm, while Chl-*b* vibrational modes are measured using 441.6 and 457.9 nm excitations [7,35]. These excitation wavelengths are located on the higher-energy side of the Soret absorption transitions of Chls (in trimeric LHCII, *ca.* 430 and 460 nm for Chl-*a* and -*b*, respectively [27]). Resonance Raman spectra of Chls contain a large number of modes delocalized over the whole conjugated dihydrophorbin macrocycle, some of which are highly sensitive to molecular conformation [44]. However, due to the large number of Chls present in LHC proteins, the diversity of Chl conformations usually induces only non-homogeneous broadening of these modes, which is difficult to interpret with any precision. Stretching modes of the conjugated carbonyls contribute in the high frequency range of the spectra (1550-1750 $cm^{-1}$): keto for Chl-*a*, and keto and formyl for Chl-*b* [45]. The frequency of these modes depends on their interaction state, and to a lesser extent on the polarity of their environment. The keto (formyl) group

stretching frequency may vary from 1700 $cm^{-1}$ (1660 $cm^{-1}$) when free from interactions in an apolar environment, to *ca.* 1660 $cm^{-1}$ (1620 $cm^{-1}$) when strongly H-bonded [7,32]. Carbonyl bands generally exhibit better separation than the other Chl modes as a result of this sensitivity, and this region is therefore one of the most informative in Chl resonance Raman spectra. The keto stretching vibration occurs along the Chl *y*-axis, and so it is strongly coupled with electronic transitions aligned along this axis ($B_y$ and $Q_y$). As a result, the resonance effect is only observed for keto vibrations when exciting into the $B_y$ transition, on the blue side. Conversely, contributions of the formyl carbonyl groups of Chl-*b* are best observed by exciting on the red side of the Soret band, where $B_X$ is the dominant transition, due to their position along the *x*-axis of the macrocycle. This was observed in chlorosome-containing BChl-*e* which, like Chl-*b,* possesses a formyl carbonyl on the *x*-axis of the molecule [46]. In these complexes, an increase in intensity of the BChl-*e* formyl carbonyl stretching mode could be observed by shifting the excitation towards the red side of the BChl-*e* Soret transition. However, the carotenoid molecules present in LHC proteins exhibit a much larger resonance Raman cross-section than Chls, and their contributions usually dominate those of Chl-*b* above 460 nm - and even at 457.9 nm. As a result, Chl-*b* contributions may become relatively difficult to observe and analyse at these wavelengths [45].

In SCP, resonance Raman spectra of Chl-*a* molecules were obtained by excitation at 413.1 nm (Fig. 5), and for Chl-*b* at 441.6 and 457.9 nm (Fig. 6). However, as can be seen in Fig. 6, Chl contributions are also observed at 488.0-nm excitation – note in particular the complex mode of the macrocycle at 1570 $cm^{-1}$, a typical frequency for the most intense resonance Raman band of Chl-*b* [45]. Moreover, the envelope of bands in the 1620-1665 $cm^{-1}$ region, corresponding to stretching modes of Chl-*b* formyl groups [35], exhibits at least three bands that coincide with modes observed at 457.9 and 441.6 nm (see Fig. 6). This is at odds with all previous measurements obtained for LHC proteins from plants and algae. For instance, the intensity of Chl-*b* contributions in these spectra are at least five times more intense than those for LHCII (Fig. S3). This anomaly cannot be explained only by the higher content of Chl-*b* in SCP, and is probably due to non-linear resonance effects. Such a phenomenon has already been described in LH1 from purple sulphur bacteria. The intensity of the carotenoid signal in the resonance Raman spectra of these complexes is unusually intense for excitations in the Soret band of BChl-*a* molecules, without any specific detectable property in their absorption spectra [33]. In the particular case of SCP, this provides a unique opportunity to observe the stretching modes of the formyl groups of the SCP-bound Chl-*b* (see below).

*3.5. Resonance Raman of SCP-bound Chl-a*

Fig. 5 displays the higher frequency region of SCP-bound Chl-*a* excited at 413.1 nm. Methine bridge stretching modes appear at 1613 $cm^{-1}$, indicating that the central magnesium atoms of SCP-bound Chl-*a* molecules are all five-coordinated [35], and their macrocycles do not experience any significant distortions. In the range corresponding to carbonyl modes, two intense contributions are observed at 1657.9 and *ca.* 1671/1677 $cm^{-1}$, together with smaller contributions at *ca.* 1692 and 1703 $cm^{-1}$. Altogether, this indicates that probably two SCP-bound Chls-*a* have their keto carbonyls involved in strong H-bonds (vibrating at 1658 $cm^{-1}$), three keto groups participate in medium-to-strong hydrogen bonds (1670-1680 $cm^{-1}$), and only one or two are free-from-interaction at higher frequencies. This pattern is somewhat similar to that observed for Chl-*a* in FCP complexes from diatoms and brown algae [7,47], and quite different from plant LHCII [35] (see Fig. 5). Note also that for SCP, we observe less weakly-bound/free-from interaction Chls-*a* than in FCP or LHCII. It is interesting to consider whether the additional free Chl-*a* keto groups in LHCII and FCP correspond to binding pockets that evolved to accommodate Chls-*b* in SCP. It has been shown that hydrogen-bonding to the Chl-*a* keto group causes a red-shift in its electronic transitions [48], and so Chls-*a* with free keto groups would tend to be on the high-energy side of the ensemble, thus on the upstream side of the energy transfer cascade. Replacement of these Chls-*a* by Chls-*b* should thus not perturb the electronic structure of the relaxed excited state of these proteins, as much as would replacing more downstream Chls-*a*.

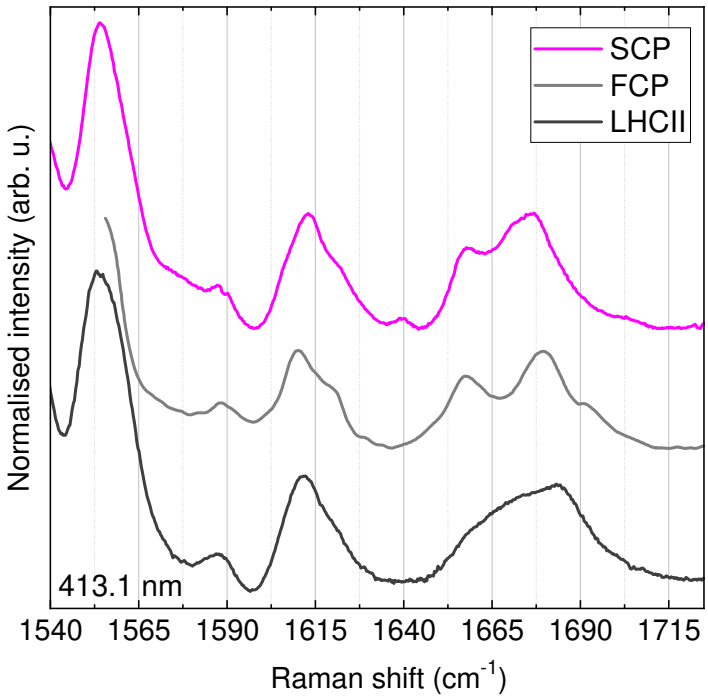


Fig. 5. 77 K resonance Raman spectra of SCP-bound Chl-*a* upon 413.1-nm excitation, in 1540-1725 $cm^{-1}$ region. FCP and LHCII are also shown for comparison.

### *3.6. Resonance Raman of SCP-bound Chl-b*

As mentioned above, SCP complexes provide a unique opportunity to determine with precision the interaction states of the formyl and keto carbonyl groups of Chl-*b* in these complexes. The contribution of keto groups (found in the 1650-1710 $cm^{-1}$ range) are expected to lose intensity when the excitation is shifted towards the red, while those of formyl groups (1620-1665 $cm^{-1}$ range) will gain intensity. This is indeed observed in Fig. 6. At 441.6 nm, the envelope of carbonyl stretching modes is complex, containing at least five major components at 1624, 1638, 1654, 1671, 1683 $cm^{-1}$, with two shoulders at *ca.* 1659 and 1698 $cm^{-1}$. At 457.9 nm excitation, all the higher frequency components (necessarily arising from keto carbonyl groups) disappear, leaving the bands from this envelope only at 1624, 1640 and 1654 $cm^{-1}$, with new bands emerging at 1630 and 1694 $cm^{-1}$ (the latter arising from the growing carotenoid contributions). In the formyl stretching range, at 488 nm excitation, five components are observed at 1622, 1630, 1638, 1655 and *ca.* 1660 $cm^{-1}$. This indicates the presence of at least four non-equivalent Chls-*b*. Taking the contributions of these formyl groups into account, the remaining contributions at 441.6 nm (which are not observed at 488.0 nm, or their intensity is much weaker than

at 441.6 nm) – at *ca*. 1654, 1671, 1683 and 1698 $cm^{-1}$ – can be attributed to Chl-*b* keto groups. Note that the bands at 1655 and *ca.* 1660 $cm^{-1}$ possibly contain a mixture of keto and formyl stretching contributions.

Higher plant LHCII, which binds six Chl-*b* molecules per monomer, exhibits three main bands in the stretching mode region of formyl carbonyls: at 1630, 1640 and 1655 $cm^{-1}$ [35] (marked as dashed lines in Fig. 6). Similar bands are observed for the SCP complex at 457.9 and 488 nm excitations, with an additional band at *ca*. 1623 $cm^{-1}$ – indicating one more population of Chl-*b* molecules in SCP. Taking into account the estimated stoichiometry of Chl-*b* in SCP, and the intensity of the observed formyl stretching bands, we estimate that two Chls-*b* possess strongly H-bonded formyl groups, with modes in the 1620-1625 $cm^{-1}$ range, two or three are involved in less strong H-bonds (1625-1635 $cm^{-1}$), two around 1640 $cm^{-1}$ are involved in medium-strength H-bonds, and one or two is free-from-interactions at *ca.* 1655 $cm^{-1}$. For Chl-*b* keto bands in SCP we assign two to three molecules having keto groups with strong H-bonds in the 1650-1665 $cm^{-1}$ region, two to three with less strong H-bonds in 1665-1675 $cm^{-1}$ range, one or two around 1685 $cm^{-1}$ are involved in medium-strength H-bonds, and one is free-from-interactions at *ca.* 1698 $cm^{-1}$.

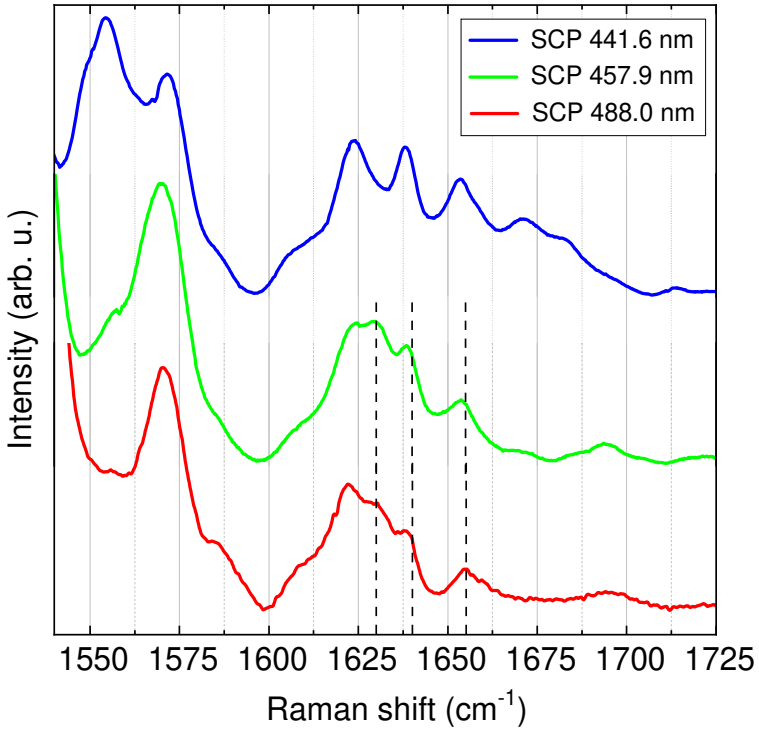


Fig. 6. 77 K Resonance Raman spectra of SCP-bound Chl-*b* upon 441.6, 457.9 and 488.0 nm excitation, in 1540-1725 $cm^{-1}$ region. Dashed lines indicate major formyl carbonyl modes previously identified for LHCIIb [35].

*3.7. Assignment of absorption transitions in SCP*

The combined information from the absorption and resonance Raman spectra can be further used to assign the absorption bands of each carotenoid pool in trimeric SCP (Table 2). The absorption band at 535 nm can be assigned to the 0-0 transition of a red-absorbing Sx. We have attributed the 0-0 transition of the other SCP-bound Sx at 501 nm, and thus its 0-1 transition must lie around 473 nm. Following the neoxanthin fingerprint modes in resonance Raman spectra, we concluded that the 0-0 position of 9'-*cis* Neo lies at 489 nm, a position close to that proposed in [36]. 489 and 462 nm thus arise from the 0-0 and 0-1 transitions of Neo, respectively. Note that the 0-1 transition of red-Sx, expected around 490 nm, could partially contribute to the 489 nm transition.

Table 2. Assignment of the carotenoid absorption transitions in SCP.

| 462 nm | 473 nm | 489 nm | 501 nm | 535 nm |
|---|---|---|---|---|
| | Sx (0-1) | Sx-red (0-1) | Sx (0-0) | Sx-red (0-0) |
| Neo (0-1) | | Neo (0-0) | | |

## 4. Conclusions

We have studied the pigment organization in trimeric SCP from the siphonous green alga *C. fragile*. We determined that the pigment stoichiometry of this light-harvesting complex is siphonaxanthin + siphonein : 9'-*cis* neoxanthin : Chl-*a* : Chl-*b* = 2.5 : 1 : 6 : 8. The combination of absorption and resonance Raman measurements at cryogenic temperatures allows us to determine that neoxanthin absorbs predominantly at 489 nm, whereas the two non-equivalent Sx/Sn molecules absorb at 501 and 535 nm. The red-shifted Sx shows a higher degree of twisting of the carbon skeleton, reminiscent of the red-shifted lutein 2 carotenoid in LHCII trimers. However, the much smaller shift of the C=C stretching mode for Sx molecules (2 $cm^{-1}$) compared to LHCII luteins (4 $cm^{-1}$) cannot account for the observed red-shift in absorption as a result of the different conformations. We hypothesise that the complex electronic structure, involving significant ICT character, is responsible for the absorption difference between the two Sx molecules in SCP.

We observe an unusual non-linear resonance effect in SCP, not previously observed for any LHC proteins from plants or algae, where the Chl-*b* contributions are unusually intense when exciting on the red side of the Soret transition. This

allows a precise analysis of H-bonding states of the formyl groups of the different Chl-*b* molecules in SCP: we observe two molecules with strongly H-bonded formyls, two to three with less-strong H-bonds, two with medium-strength H-bonds, and one or two with free-from-interaction formyl groups. For Chl-*b* keto bands we assign two to three molecules having keto groups with strong H-bonds, two to three with less strong H-bonds, one or two involved in medium-strength H-bonds, and one free-from-interactions. The analysis of Chl-*a* keto groups reveals two keto carbonyls involved in strong H-bonds, three keto groups with medium-to-strong hydrogen bonds, and only one or two free-from-interaction keto groups. SCP exhibits fewer free Chl-*a* keto groups than other LHC proteins. We speculate that these sites specifically evolved to accommodate the extra Chls-*b* in SCP, as the replacement of Chls-*a* possessing free keto groups by Chls-*b* should not dramatically influence the electronic structure of the relaxed excited state of the protein.

**Acknowledgement**

This work was supported by the platform of Biophysics of I2BC supported by French Infrastructure for Integrated Structural Biology (FRISBI) ANR-10-INBS-05-05, the European Union's Horizon 2020 research and innovation program under the Marie Skłodowska-Curie grant agreement No 675006 (SE2B), and Gilibert project S-LZ-19-3. We would like to thank Dr. Nami Yamano (The OCU Advanced Research Institute for Natural Science and Technology, Osaka City University, Japan; present address, Ren Min University of China, Beijing, P.R. China) for her contribution to prepare a pigment, siphonaxanthin. We also thank a past master course student Mr. Ryuichi Kano (Graduate School of Science, Osaka City University) for his contribution to cultivate *Codium fragile*. We also thank Dr. Masahiko Iha (South Product Co. Ltd., Okinawa, Japan) for providing cultivated *Codium intricatum*.

**References**

[1] B. Demmig, K. Winter, A. Krüger, F.-C. Czygan, Photoinhibition and Zeaxanthin Formation in Intact Leaves: A Possible Role of the Xanthophyll Cycle in the Dissipation of Excess Light Energy, Plant Physiol., 84 (1987) 218–224.

[2] B. Demmig-Adams, Carotenoids and photoprotection in plants: A role for the xanthophyll zeaxanthin, BBA - Bioenerg., 1020 (1990) 1–24.

[3] Z. Liu, H. Yan, K. Wang, T. Kuang, J. Zhang, L. Gui, X. An, W. Chang, Crystal structure of spinach major light-harvesting complex at 272 Å resolution, Nature, 428 (2004) 287–292.

[4] S. Streckaite, Z. Gardian, F. Li, A.A. Pascal, R. Litvin, B. Robert, M.J. Llansola-

Portoles, Pigment configuration in the light-harvesting protein of the xanthophyte alga *Xanthonema debile*, Photosynth. Res., 138 (2018).
[5] M.J. Llansola-Portoles, R. Litvin, C. Ilioaia, A.A. Pascal, D. Bina, B. Robert, Pigment structure in the violaxanthin–chlorophyll-*a*-binding protein VCP, Photosynth. Res., 134 (2017) 51–58.
[6] M.J. Llansola-Portoles, C. Uragami, A.A. Pascal, D. Bina, R. Litvin, B. Robert, Pigment structure in the FCP-like light-harvesting complex from *Chromera velia*, Biochim. Biophys. Acta - Bioenerg., 1857 (2016) 1759–1765.
[7] A.A. Pascal, L. Caron, B. Rousseau, K. Lapouge, J.C. Duval, B. Robert, Resonance Raman spectroscopy of a light-harvesting protein from the brown alga *Laminaria saccharina*, Biochemistry, 37 (1998) 2450–2457.
[8] L. Premvardhan, L. Bordes, A. Beer, C. Büchel, B. Robert, Carotenoid structures and environments in trimeric and oligomeric fucoxanthin chlorophyll *a/c2* proteins from resonance raman spectroscopy, J. Phys. Chem. B, 113 (2009) 12565–12574.
[9] W. Wang, L.J. Yu, C. Xu, T. Tomizaki, S. Zhao, Y. Umena, X. Chen, X. Qin, Y. Xin, M. Suga, G. Han, T. Kuang, J.R. Shen, Structural basis for blue-green light harvesting and energy dissipation in diatoms, Science , 363 (2019).
[10] C. Bonetti, M.T.A. Alexandre, I.H.M. Van Stokkum, R.G. Hiller, M.L. Groot, R. Van Grondelle, J.T.M. Kennis, Identification of excited-state energy transfer and relaxation pathways in the peridinin-chlorophyll complex: An ultrafast mid-infrared study, Phys. Chem. Chem. Phys., 12 (2010) 9256–9266.
[11] D. Zigmantas, R.G. Hiller, F.P. Sharples, H.A. Frank, V. Sundström, T. Polívka, Effect of a conjugated carbonyl group on the photophysical properties of carotenoids, Phys. Chem. Chem. Phys., 6 (2004) 3009–3016.
[12] W. Wang, X. Qin, M. Sang, D. Chen, K. Wang, R. Lin, C. Lu, J.R. Shen, T. Kuang, Spectral and functional studies on siphonaxanthin-type light-harvesting complex of photosystem II from *Bryopsis corticulans*, Photosynth. Res., 117 (2013) 267–279.
[13] E.E. Benson, A.H. Cobb, Pigemnt/Protein complexes of the intertidal algae *Codium fragile*, New Phytol., 95 (1983) 581–594.
[14] J.M. Anderson, Chlorophyll-protein complexes of a Codium species, including a light-harvesting siphonaxanthin-Chlorophyll *a/b*-protein complex, an evolutionary relic of some Chlorophyta, Biochim. Biophys. Acta, 724 (1983) 370–380.
[15] J.M. Anderson, Chlorophyll-protein complexes of a marine green alga, Codium species (Siphonales), Biochim. Biophys. Acta, 806 (1985) 145–153.
[16] C. Uragami, D. Galzerano, A. Gall, Y. Shigematsu, M. Meisterhans, N. Oka, M. Iha, R. Fujii, B. Robert, H. Hashimoto, Light-dependent conformational change of neoxanthin in a siphonous green alga, *Codium intricatum*, revealed by Raman spectroscopy, Photosynth. Res., 121 (2014) 69–77.
[17] K. Nakayama, M. Okada, Purification and Characterization of Light-Harvesting Chlorophyll *a*/*b*-Protein Complexes of Photosystem II from the Green alga, *Bryopsis maxima*, 31 (1990) 253–260.
[18] G. Chen, X. Niu, X. Chen, L. Li, T. Kuang, S. Li, Characterization of chlorophyll-protein complexes isolated from a Siphonous green alga, *Bryopsis corticulans*, Photosynth. Res., 96 (2008) 75–81.
[19] J.M. Anderson, J. Barrett, Light-Harvesting Pigment-Protein Complexes of Algae, in: L.A. Staehelin, C.J. Arntzen (Eds.), Photosynth. III. Photosynth.

Membr. Light Harvest. Syst., Springer-Verlag Berlin Heidelberg GmbH, 1986: pp. 269–285.
[20] P. Akhtar, P.J. Nowakowski, W. Wang, T.N. Do, S. Zhao, G. Siligardi, G. Garab, J.-R. Shen, H.-S. Tan, P.H. Lambrev, Spectral tuning of light-harvesting complex II in the siphonous alga *Bryopsis corticulans* and its effect on energy transfer dynamics, BBA - Bioenerg., 1861 (2020) 148191.
[21] L. Provasoli, Growing marine seaweeds, in: Proc. 4th Int. Seaweed Symp., Pergamon Press, Oxford, 1963: pp. 9–17.
[22] R. Fujii, N. Yamano, H. Hashimoto, N. Misawa, K. Ifuku, Photoprotection vs photoinhibition of photosystem II in transplastomic lettuce (*Lactuca sativa*) dominantly accumulating astaxanthin, Plant Cell Physiol., 57 (2016) 1518–1529.
[23] A. De Martino, D. Douady, B. Rousseau, J.C. Duval, L. Caron, M. Vegetales, Characterization of Two Light-Harvesting Subunits Isolated from the Brown Alga *Pelvetia canaliculata*: Heterogeneity of Xanthophyll Distribution, Photochem. Photobiol., 66 (1997) 190–197.
[24] S. Caffarri, R. Kouril, S. Kereiche, E.J. Boekema, R. Croce, Functional architecture of higher plant photosystem II supercomplexes, EMBO J., 28 (2009) 3052–3063.
[25] S. Akimoto, I. Yamazaki, A. Murakami, S. Takaichi, M. Mimuro, Ultrafast excitation relaxation dynamics and energy transfer in the siphonaxanthin-containing green alga *Codium fragile*, Chem. Phys. Lett., 390 (2004) 45–49.
[26] S. Akimoto, T. Tomo, Y. Naitoh, A. Otomo, A. Murakami, M. Mimuro, Identification of a new excited state responsible for the in vivo unique absorption band of siphonaxanthin in the green alga *Codium fragile*, J. Phys. Chem. B, 111 (2007) 9179–9181.
[27] H. Scheer, An Overview of Chlorophylls and Bacteriochlorophylls: Biochemistry, Biophysics, Functions and Applications, in: B. Grimm, R.J. Porra, W. Rudiger, H. Scheer (Eds.), Chlorophylls and Bacteriochlorophylls, Springer, 2006: pp. 1–26.
[28] P.W. Hemelrijk, S.L.S. Kwa, R. van Grondelle, J.P. Dekker, Spectroscopic properties of LHC-II, the main light-harvesting chlorophyll *a/b* protein complex from chloroplast membranes, BBA - Bioenerg., 1098 (1992) 159–166.
[29] E.J. Peterman, F.M. Dukker, R. van Grondelle, H. van Amerongen, Chlorophyll *a* and carotenoid triplet states in light-harvesting complex II of higher plants, Biophys. J., 69 (1995) 2670–2678.
[30] M. Lutz, J. Breton, Chlorophyl association in the chloroplast: resonance Raman spectroscopy, Biochem. Biophys. Res. Commun., 53 (1973) 413–418.
[31] B. Robert, Resonance Raman Studies in Photosynthesis – Chlorophyll and Carotenoid Molecules, in: J. Amesz, A.J. Hoff (Eds.), Biophys. Tech. Photosynth., Kluwer Academic Publishers, 1996: pp. 161–176.
[32] B. Robert, S. De Biophysique, The Electronic Structure , Stereochemistry and Resonance Raman Spectroscopy of Carotenoids, Photochem. Carotenoids, (1999) 189–201.
[33] B. Robert, M. Lutz, Structures of antenna complexes of several Rhodospirillales from their resonance Raman spectra, BBA - Bioenerg., 807 (1985) 10–23.
[34] A. V. Ruban, A.A. Pascal, B. Robert, P. Horton, Configuration and dynamics of xanthophylls in light-harvesting antennae of higher plants: Spectroscopic analysis of isolated light-harvesting complex of photosystem II and thylakoid

membranes, J. Biol. Chem., 276 (2001) 24862–24870.
[35] A. Pascal, U. Wacker, K.D. Irrgang, P. Horton, G. Renger, B. Robert, Pigment binding site properties of two photosystem II antenna proteins: A resonance Raman investigation, J. Biol. Chem., 275 (2000) 22031–22036.
[36] A. V. Ruban, A.A. Pascal, B. Robert, Xanthophylls of the major photosynthetic light-harvesting complex of plants: Identification, conformation and dynamics, FEBS Lett., 477 (2000) 181–185.
[37] M.M. Mendes-Pinto, E. Sansiaume, H. Hashimoto, A.A. Pascal, A. Gall, B. Robert, Electronic absorption and ground state structure of carotenoid molecules, J. Phys. Chem. B, 117 (2013) 11015–11021.
[38] L. Rimai, Vibrational Spectra of Some Carotenoids and Related Linear Polyenes A Raman Spectroscopic Study, Atlas Vib. Spectra Liq. Cryst., 4560 (1973) 11–22.
[39] M. Macernis, D. Galzerano, J. Sulskus, E. Kish, Y.H. Kim, S. Koo, L. Valkunas, B. Robert, Resonance Raman spectra of carotenoid molecules: Influence of methyl substitutions, J. Phys. Chem. A, 119 (2015) 56–66.
[40] M.M. Mendes-Pinto, D. Galzerano, A. Telfer, A.A. Pascal, B. Robert, C. Ilioaia, Mechanisms underlying carotenoid absorption in oxygenic photosynthetic proteins, J. Biol. Chem., 288 (2013) 18758–18765.
[41] S. Saito, Normal coordinate analysis of p-nitrobenzaldehyde and assignments of infrared and Raman bands, J. Raman Spectrosc., 20 (1983) 263–266.
[42] B. Robert, Resonance Raman spectroscopy, Photosynth. Res., 101 (2009) 147–155.
[43] H. Yan, P. Zhang, C. Wang, Z. Liu, W. Chang, Two lutein molecules in LHCII have different conformations and functions: Insights into the molecular mechanism of thermal dissipation in plants, Biochem. Biophys. Res. Commun., 355 (2007) 457–463.
[44] M. Fujiwara, M. Tasumi, Metal-sensitive bands in the Raman and infrared spectra of intact and metal-substituted chlorophyll *a*, J. Phys. Chem., 90 (1986) 5646–5650.
[45] M. Lutz, Antenna chlorophyll in photosynthetic membranes A study by resonance Raman spectroscopy, BBA - Bioenerg., 460 (1977) 408–430.
[46] U. Feiler, D. Albouy, M. Lutz, B. Robert, Pigment interactions in chlorosomes of various green bacteria, Photosynth. Res., 41 (1994) 175–180.
[47] L. Premvardhan, B. Robert, A. Beer, C. Büchel, Pigment organization in fucoxanthin chlorophyll *a/c2* proteins (FCP) based on resonance Raman spectroscopy and sequence analysis, Biochim. Biophys. Acta - Bioenerg., 1797 (2010) 1647–1656.
[48] M.J.M.J. Llansola-Portoles, F. Li, P. Xu, S. Streckaite, C. Ilioaia, C. Yang, A. Gall, A.A.A. Pascal, R. Croce, B. Robert, Tuning antenna function through hydrogen bonds to chlorophyll *a*, Biochim. Biophys. Acta - Bioenerg., (2019) 148078.